Available online at www.sciencedirect.com
ScienceDirect
Dyes and Pigments 79 (2008) 145–152
DYES and PIGMENTS
www.elsevier.com/locate/dyepig

Cooperative enhancement of two-photon absorption based on electron coupling in triphenylamine-branching chromophore

Zhiming Wang [a], Xiaomei Wang [a,*], Junfang Zhao [b], Wanli Jiang [c], Ping Yang [a], Xiangyun Fang [b,**], Maoyi Zhou [a], Manhuan Cheng [a]

[a] *Institute of Material Science and Engineering, Department of Chemistry, Suzhou University, Suzhou 215021, China*
[b] *Laboratory of Ultra-Fast Laser, Technical Institute of Physics and Chemistry, Chinese Academy of Sciences, Beijing, China*
[c] *State Key Laboratory of Crystal Materials, Shandong University, Jinan, China*

Received 13 December 2007; received in revised form 25 January 2008; accepted 29 January 2008
Available online 13 February 2008

Abstract

Two novel, triphenylamine derivatives *N*-(4-(4-(diphenylamino)styryl)phenyl)acetamide and *N*-(4-(4-(bis-(4-(4-(diphenyl-amino)styryl)phenyl)amino)styryl)phenyl)acetamide were synthesized. The two-photon absorption of *N*-(4-(4-(bis-(4-(4-(diphenyl-amino)styryl)phenyl)amino)-styryl)phenyl) was ~17-fold greater relative to *N*-(4-(4-(diphenylamino)styryl)phenyl)acetamide. Linear absorption spectra, steady-fluorescence and time-resolved fluorescence spectra revealed that electron coupling originating from π-electron delocalization is responsible for the strong cooperative enhancement of TPA within the compounds. This is confirmed by the Lippert-Mataga equation.
© 2008 Elsevier Ltd. All rights reserved.

Keywords: Two-photon absorption; Two-photon induced fluorescence; Triphenylamine-branching chromophore; Electron coupling; Dipole moment difference; Excited electron delocalization

1. Introduction

Molecular two-photon absorption (TPA) has gained interest over recent years owing to the applications in various fields, including two-photon excited fluorescence microscopy [1], three-dimensional microfabrication [2–4], high-density optical data storage [5,43–45], up-converted lasing [6], optical-limiting [7] and photodynamic therapy [8]. Till now, the molecular optimization for TPA material has largely focused on one-dimensional dipolar [9,10], quadrupolar [11–18], octupolar [19–21] and multibranched chromophores [22–24]. It is known that large TPA cross-section roots in either electron coupling [25] or vibration coupling [26] within multibranched systems. The former effect is much larger than the latter one with respect to the cooperative enhancement of TPA. Therefore, the research of electron coupling effect upon enhanced TPA is now attracting increasing attention [27,28]. Herein, two new triphenylamine derivatives *N*-(4-(4-(diphenylamino)styryl)phenyl)acetamide (abbreviated as monobranch **1**) and *N*-(4-(4-(bis-(4-(4-(diphenylamino)styryl)phenyl)amino)styryl)phenyl)acetamide (abbreviated as multibranch **2**) have been synthesized and characterized. These dyes possess the bridge of stilbene flanked on one side by acetamide group for the purpose of packing metal nanoparticles later. The other terminal was capped with diphenylamine and bis(4-(4-(diphenylamino)styryl)phenyl)amine, respectively, in order to investigate the influence of multibranch architecture upon TPA cooperative enhancement. Linear optical properties including absorption, steady state fluorescence and time-resolved fluorescence spectra are comparatively studied. Two-photon absorption (TPA) properties were measured by two-photon induced fluorescence (TPF) method, using Ti:sapphire femtosecond laser pulse in the range of 700–880 nm. It was found that relative to monobranch **1**, multibranch **2** displays the significant increase in two-photon absorption cross-section with

* Corresponding author. Tel.: +86 512 62092786; fax: +86 512 67246786.
** Corresponding author.
E-mail address: wangxiaomei@suda.edu.cn (X. Wang).

0143-7208/$ - see front matter © 2008 Elsevier Ltd. All rights reserved.
doi:10.1016/j.dyepig.2008.01.015

the concomitance of remarkable bathochromic shift of two-photon fluorescence (TPF) peak. Optimization conformation obtained by Hyperchem program shows that multibranch **2** with three triphenylamine units lies in one common plane and Lippert–Mataga equation confirms that multibranch **2** exhibits much larger dipole moment difference ($\Delta\mu_{ge}$) between the ground and excited states than monobranch **1**. This indicates that multibranched system might show larger intramolecular excited charge transfer. The obtained results strongly support the opinions that multibranch **2** exhibits large π-electron delocalization and TPA cooperative enhancement owing to electron coupling effect.

2. Materials and measurements

2.1. Materials

Both samples possess the characteristics of stilbene as π-bridge end-capped with the same acetamide group as one terminal, while varying the other terminals such as diphenylamine group for monobranch **1** and multibranched diphenylamine group for multibranch **2**. The synthesis routes for both samples are shown in Scheme 1.

2.2. Synthesis

2.2.1. N-Phenyl-N-(4-vinylphenyl)benzenamine (compound *2*)

4-(Diphenylamino) benzaldehyde (compound **1**) [29] (3.64 g, 13.3 mmol) and methyl triphenylphosphonium iodide [42] (10.64 g, 26.3 mmol) were dissolved in 50 mL of dry tetrahydrofuran. To this solution was added 2.5 g (105 mmol) of sodium hydride as strong base at room temperature. The mixture was refluxed for 6 h under the nitrogen atmosphere and then poured into excess distilled water. The precipitate was recrystallized in methanol to give 1.4 g of compound **2** (84%). Melting point 85–88 °C. Mass spectrum (*m/z*): 271.1338 (M^+, 100%). ^{1}H NMR (400 MHz, $CDCl_3$) *δ*: 5.143, 5.170 (d, 1H, *J* 10.8 Hz), 5.619, 5.663 (d, 1H, *J* 17.6 Hz), 6.625–6.696 (m, 1H), 7.004, 7.025 (d, 2H, *J* 8.4 Hz), 7.168–7.362 (m, 10H), 7.666, 7.687 (d, 2H, *J* 8.4 Hz).

2.2.2. N-(4-Bromophenyl)acetamide (compound *4*)

A flask fitted with magnetic stirrer and condenser was charged with 2.0 g (11.6 mmol) 4-bromobenzenamine (compound **3**), 5.43 g (5 mL) of acetic anhydride in the presence of acetic acid (1.35 g, 23 mmol) under nitrogen. The reaction was refluxed for 10 h and then cooled to room temperature.

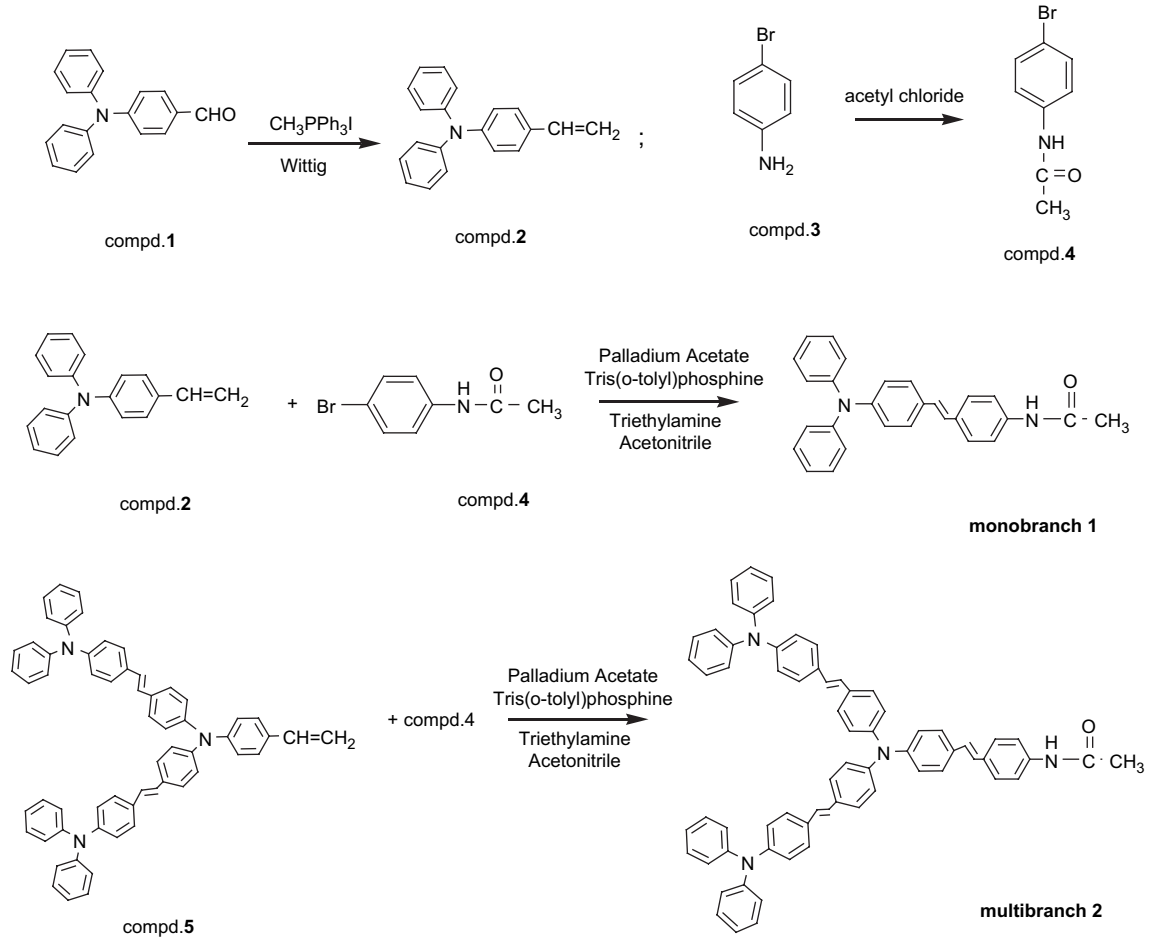

Scheme 1. The synthesis routes of monobranch **1** and multibranch **2**.

The white powder was filtered and recrystallized in acetic anhydride to give compound **4** as white crystals with yield 70%. Melting point 167–168 °C. ^{1}H NMR ($CDCl_3$ 400 MHz) δ: 2.143 (s, 3H, CH_3), 7.32 (2H, d, J 8.4 Hz), 7.42 (2H, d, J 8.4 Hz).

2.2.3. N-(4-(4-(diphenylamino)styryl)phenyl) acetamide (monobranch *1*)

Under the anhydrous and oxygen-free conditions, 1 g (3.7 mmol) of *N*-phenyl-*N*-(4-vinylphenyl)benzenamine (compound **2**), 0.79 g (3.7 mmol) of *N*-(4-bromophenyl)acetamide (compound **4**) and a small amount of tris(*o*-tolyl)phosphine and palladium acetate in the presence of solvent were stirred in the flask at 85 °C for 22 h under argon atmosphere. Then solvent was removed by evaporation and the slurry was purified through chromolographic column on silica gel by using pure chloroform as eluent. Pale green powders were obtained in yield 58% and melting point 240 °C. ν (KBr)/cm^{-1}: 3440.7 (N–H), 3055.1, 3032.1 (=C–H), 2924.8 ($-CH_3$), 2853.3 ($-CH_2-$), 1659.5 (C=O), 1638.0 (C=C), 1590.4, 1519.0, 1492.1 (Ar–), 821 (*trans*-CH=CH–). Mass spectrum (*m/z*): 404.168 (M^+, 100%). ^{1}H NMR ($CDCl_3$, 400 MHz) δ: 2.206 (s, 3 H), 7.054 (d, 2H, J 8.8 Hz), 7.118 (d, 2H, J 8.0 Hz), 7.276 (m, 10H), 7.369 (s, 1H), 7.390 (s, 1H), 7.456 (d, 2H, J 8.0 Hz), 7.499 (d, 2H, J 7.6 Hz).

2.2.4. N-(4-(4-(Bis(4-(4-(diphenylamino)styryl)phenyl) amino)styryl)phenyl)acetamide (multibranch *2*)

By replacing compound **2** with compound **5** [30], multibranch **2** can be obtained using the similar method as monobranch **1**. To get the pure product, repeated chromolographic column separations have been conducted. Pale green powders were obtained in yield 41% and melting point 118–120 °C. ν (KBr)/cm^{-1}: 3445.4 (N–H), 3061.6, 3030.6 (=C–H), 2961.6, 2925.2 ($-CH_3$), 2854.3 ($-CH_2-$), 1664.9 (C=O), 1636.5 (C=C), 1595.7, 1535.3, 1507.5 (Ar–), 821 (*trans*-CH=CH–). MS *m/z* Calcd: 943, Found: 944. ^{1}H NMR ($CDCl_3$, 400 MHz) δ: 2.194 (s, 3H), 7.018–6.958 (m, 18H), 7.083–7.063 (m, 14H), 7.222–7.203 (m, 10H), 7.302, 7.282 (d, 2H, J 8 Hz), 7.317, 7.290 (d, 2H, J 10.8 Hz), 7.366, 7.345 (d, 2H, J 8.4 Hz), 7.405, 7.380 (d, 2H, J 10 Hz).

2.3. Measurements

IR spectra were measured by Nicolet FT-IR 5DX instrument. Electron impact (Mode laser) mass spectra were obtained on 4700 Proteome Analyzer (MALDI-TOF-TOF) produced by ABI Company. And EI mass spectra were obtained on HP 5989 mass spectra instruments. Nuclear magnetic resonance spectra were determined on GCT-TOF NMR spectrometer.

Linear absorption measurements have been measured by a Hitachi U-3500 spectra-photometer with 2-nm resolution. The influences from the quartz liquid cell and the solvent have been subtracted. One-photon fluorescence spectra including steady state fluorescence spectra and time-resolved decay curves were measured by an Edinburgh FLS 920 fluorophotometer in a 1-cm path length cell.

Two-photon absorption (TPA) cross-sections (δ_{TPA}) of samples (in THF at 1.0×10^{-4} mol dm^{-3}) were obtained by two-photon fluorescence (TPF) method [31] at femtosecond laser pulse using Ti:sapphire system (700–880 nm, 80 MHz, <130 fs) as the light source, according to Eq. (1),

$$\delta_{TPA} = \delta_{TPA}(\text{ref})\frac{\Phi_r F_s n_r c_r}{\Phi_s F_r n_s c_s} \quad (1)$$

where the subscripts "s" and "r" represent sample and reference (here fluorescein in sodium hydroxide aqueous solution at concentration of 1.0×10^{-4} mol dm^{-3} was used as reference), respectively. F is the overall TPF signal collected by the fiber spectra meter. Φ, n and c are the OPF quantum yield, refractive index of solvent and the concentration of solution, respectively. Since The TPF quantum yield (Φ_{TPF}) measurement is far more difficult and the luminescence behaviors on OPF and TPF are similar, i.e., the emission from the first excited state (S_1) to the ground state (S_0) [32], one might suppose that $\Phi_{TPF} \approx \Phi_f$. The OPF quantum yield (Φ_f) of two samples were measured using fluorescein (in 0.1 mol dm^{-3} aqueous NaOH) as a standard and presented in Table 1.

3. Results and discussion

3.1. Linear photophysical properties

Linear absorption and one-photon fluorescence (OPF) spectra of two samples in different solvents are shown in Fig. 1. As can be seen that the maximum absorption peaks show about 14-nm red-shift from monobranch **1** (λ_{max}^{ab} = 366 nm, THF) to multibranch **2** (λ_{max}^{em} = 380 nm, THF). At the same time, the OPF peak shows 22-nm of red-shift from monobranch **1** (λ_{max}^{em} = 438 nm, THF) to multibranch **2** (λ_{max}^{em} = 460 nm, THF) under the excitation with respective maximum absorption wavelength. It is found that monobranch **1** possesses much higher fluorescence intensity than multibranch **2**; moreover, monobranch **1** gives stronger fluorescence emission in polar solvents (i.e., DMF, ethyl acetate and THF) than that in apolar solvent (i.e., toluene). On the contrary, the fluorescence intensities of multibranch **2** gradually decrease with increasing solvent polarity from toluene to THF, ethyl acetate, and DMF. These results indicate that monobranch **1** displays similar to symmetric chromophore [32], while multibranch **2** shows the asymmetric chromophore's behavior [33].

Optimized conformations of monobranch **1** and multibranch **2**, obtained by Hyperchem program, display the stilbene subunits in both samples being planar (see Fig. 2).

Table 1
One-photon and two-photon property of samples in THF

	λ_{max}^{OPA}, nm	λ_{max}^{OPF}, nm	Φ_f	τ, ns	λ_{max}^{TPF}, nm	δ, GM
Monobranch **1**	366	438	0.33	1.67	440	91
Multibranch **2**	380	460	0.31	1.56, 6.47	487	1562

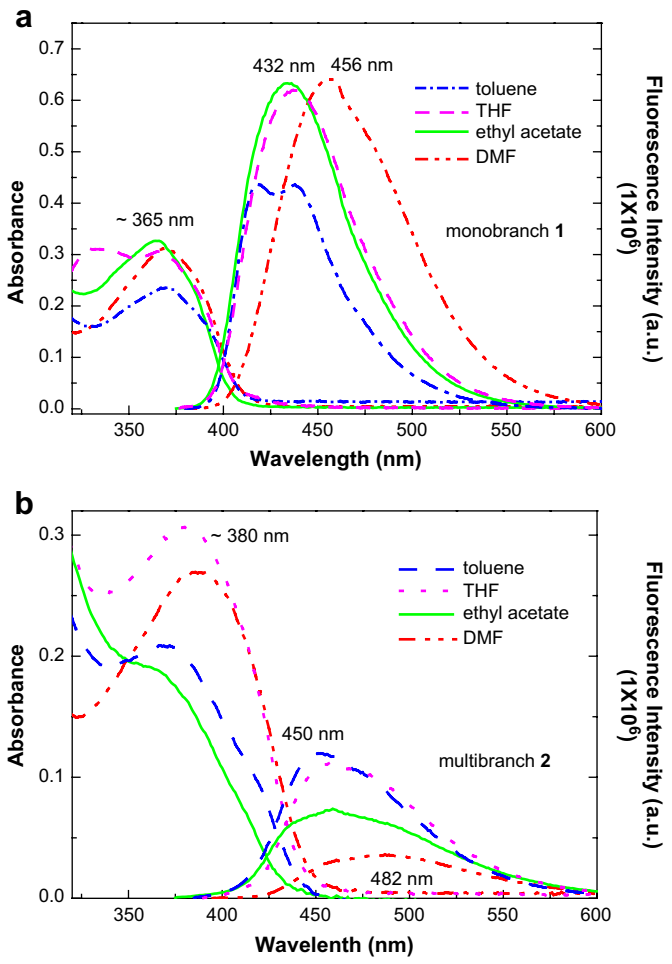

Fig. 1. Linear absorption (a) and one-photon fluorescence (b) spectra of two samples in different solvents at 1×10^{-5} mol dm^{-3}.

Strangely, the triphenylamine subunit on the terminal of monobranch **1** adopts the propeller-shaped, while the three of triphenylamine subunits in multibranch **2** lie in one common plane that is in agreement with the crystallographic data in BDPAS (*E*-4,4'-bis(diphenylamino)stilbene) [34] and in triphenylamine [35,36]. This can be explained by the sp^2-hybridization of nitrogen and resulting effective electron delocalization within entire molecular skeleton [37]. As a result, linear absorption spectra of multibranch **2** exhibit the obvious red-shift, as presented in Fig. 1(b). On the other hand, although multibranch **2** shows the planar configuration, its fluorescence intensity is dramatically decreased relative to monobranch **1**, strongly suggesting that the skeleton of multibranch **2** is flexible and easy to twist, which might consume more excited energy and reduces the fluorescence intensity. On the other hand, the flexible and twisted multibranch **2** behaves similar to asymmetric chromophore and shows the corresponding solvent effects.

3.2. Nonlinear photophysical properties

Two-photon fluorescence (TPF) spectra of two samples at different pumped powers are presented in Fig. 3. As shown in the inset of Fig. 3, when the pumped powers are increased from 36 to 97 mW, the values 1.65−1.75 of the logarithmic plots of the fluorescence integral versus pumped powers are away from 2, which suggests some kind of saturation existence. In order to eliminate saturation photophysical processes and ensure the two-photon excited fluorescence intensity being quadratically dependent on excitation intensity, the excitation powers in our TPA cross-section measurements are limited below 45 mW. Thus, the slopes of ~1.9 for

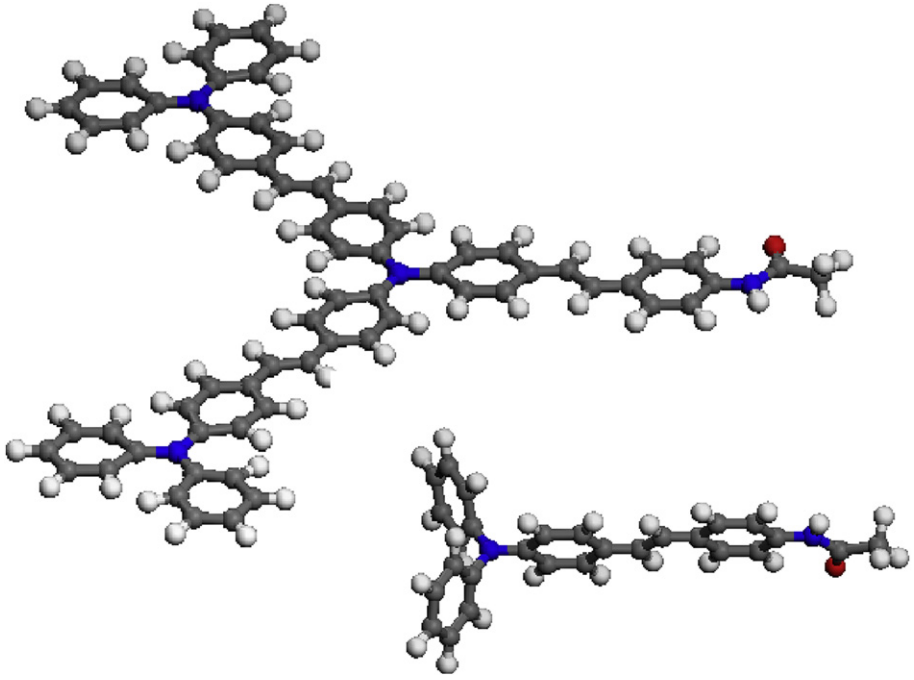

Fig. 2. Optimized geometry of monobranch **1** and multibranch **2**.

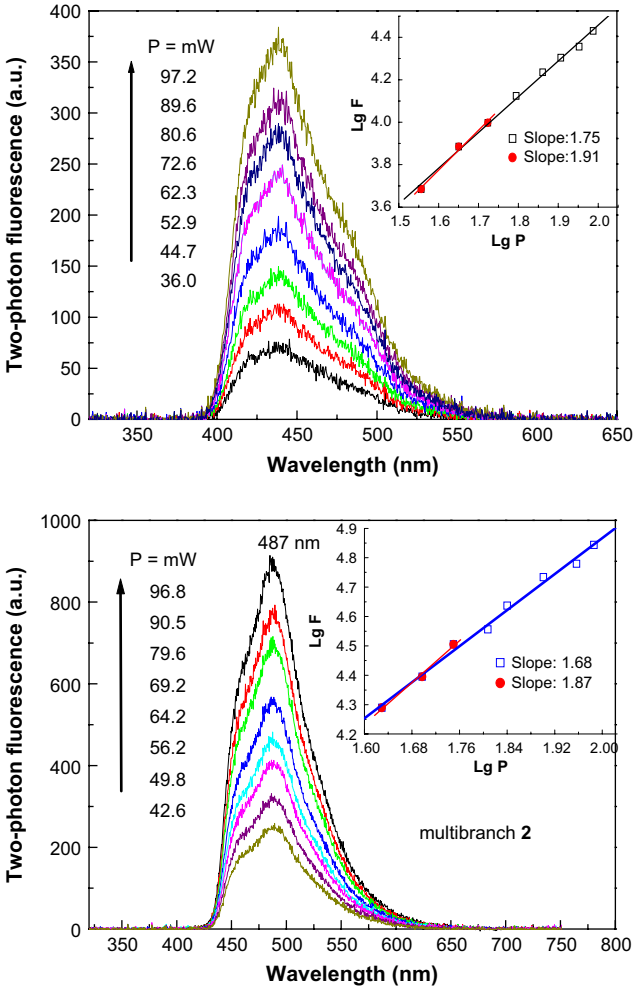

Fig. 3. Two-photon excited fluorescence spectra of samples under different pumped powers at 800 nm (1×10^{-4} mol dm^{-3}, THF).

monobranch **1** and multibranch **2** are obtained in the logarithmic plots of the fluorescence integral versus excitation intensity (shown in Fig. 3, inset), which is in agreement with the theoretical value [31]. One can notice that the wavelengths of two-photon fluorescence peaks are at 440 nm for monobranch **1** and at 487 nm for multibranch **2**. The red-shift of TPF peak is due to the reabsorption of relatively concentrated solution (1×10^{-4} mol dm^{-3}) used in two-photon fluorescence (TPF) measurements, compared to dilute solution (1×10^{-5} or 1×10^{-6} mol dm^{-3}) used in one-photon fluorescence (OPF) measurements. Additionally, the TPF spectra in structured form suggest that OPF and TPF emissions are from the different vibrational states at the first excited electron state (S_1). Comparing Fig. 1 with Fig. 3, one can notice that from monobranch **1** to multibranch **2**, the one-photon fluorescence gives 22-nm of red-shift, while two-photon fluorescence exhibits 47-nm of red-shift (see Table 1). This fact suggests that the ultrafast laser induces the excited state of multibranch **2** to be more stable; meanwhile, strong π-electron delocalization and resulting the electron coupling within entire conjugated system might occurs [23,36]. The TPF intensity of multibranch **2** shows almost three times as strong as that of monobranch **1** at the same pumped power (see Fig. 3), implying that multibranch **2** with π-electron delocalization and the electron coupling has effective contribution to enhance two-photon process.

Two-photon absorption (TPA) excited spectra, shown in Fig. 4, were obtained by Ti:sapphire femtosecond laser system according to two-photon fluorescence method [31]. In our TPA cross-section measurement, the low frequency (1 kHz) femtosecond laser pulses were used as excitation source and the excitation powers were limited below 45 mW. The experimental uncertainty for the calculation of the TPA cross-section is estimated to be about 10%, by the comparison of the TPA cross-section of fluorescein between our measurement and reported data [31]. Due to the limitation of our detecting equipment, we cannot observe the two-photon absorption (TPA) peaks of both samples but expect that their strong TPA peaks may exist shorter than 700 nm, as can be seen in Fig. 4. And monobranch **1** possesses the TPA cross-section less than 100 GM ($1\ \mathrm{GM} = 1 \times 10^{-50}\ \mathrm{cm^4\ s\ photon^{-1}}$) in the range of 700–880 nm, while multibranch **2** possesses the maximum TPA cross-section as high as 1562 GM, showing about 17-fold increase relative to monobranch **1**. Evidently, the electron delocalization (electron coupling) through planar and flexible configuration results in strong cooperative enhancement of two-photon absorption in branching structure. This cooperative enhancement effect can also be confirmed by time-resolved fluorescence decay curves, presented in Fig. 5, wherein monobranch **1** gives rise to quasi-monoexponential fit and exhibits the lifetime of 1.67 ns, which is close to the BDPAS lifetime [38]. Meanwhile, multibranch **2** gives rise to dual exponential fit and exhibits the dual lifetimes of 1.56 and 6.47 ns. The presence of the faster component (content of 64%) is comparable to the decay time of BDPAS [38], while the presence of a slow decay component (content of 36%) is clear evidence of the presence of interactions (i.e., electron coupling) among the individual branch segments.

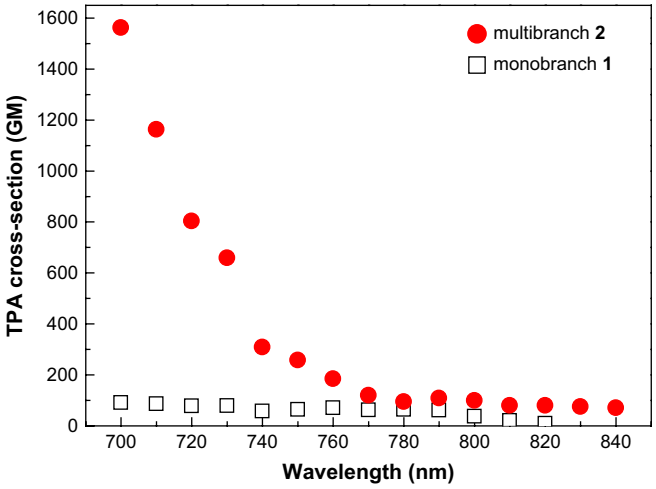

Fig. 4. Two-photon excited spectra of samples, pumped by femtosecond laser pulse at 700–840 nm (1×10^{-4} mol dm^{-3}, THF).

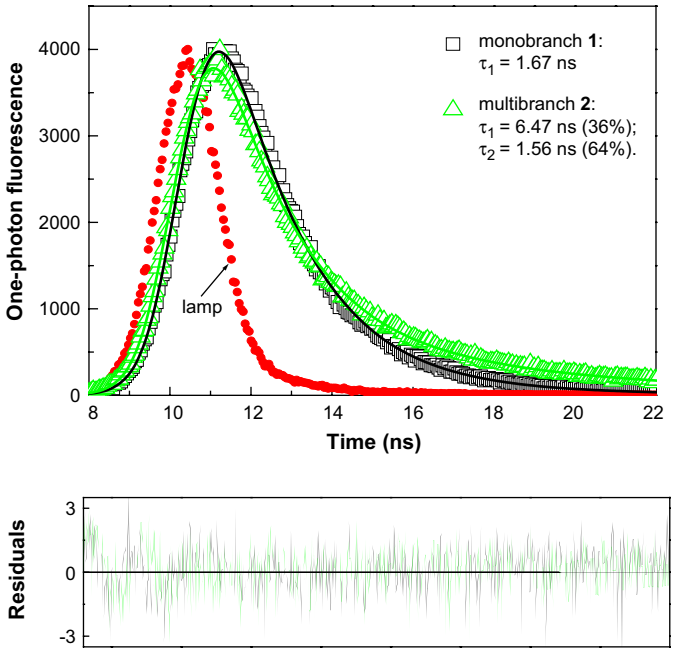

Fig. 5. Decay curves of samples in which the solid lines are the fitting results of the corresponding lifetime.

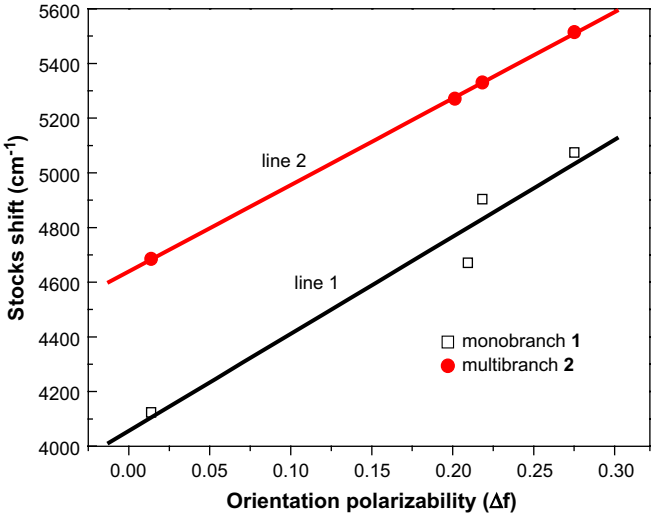

Fig. 6. The relationship between Stoke's shift ($\Delta\nu$) and orientation polarizability (Δf) of solvents for two samples.

The fact that the long time component appears with concomitance of short time component decreasing implies the existence of more delocalized relaxed state or interaction state between individual branches. Such electron coupling and excitation delocalization contribute to a significant hindrance to conformation relaxation processes thus leading to elongation of the fluorescence decay time [39–41].

Generally, electron coupling interaction responds to large excitation delocalization and presents larger dipole moment difference ($\Delta\mu_{ge} = \mu_e - \mu_g$) between the ground and excited state. According to Lippert–Mataga equation, Stokes shift ($\Delta\nu$) is direct ratio of the dipole moment difference ($\Delta\mu_{ge}$) of sample and the orientation polarizability (Δf) of solvents, and is inverse ratio of the cavity radius (α) of sample, as shown in Eq. (2):

$$\Delta\nu = \frac{\Delta\mu_{ge}^2}{c\hbar\alpha^3}\Delta f + C \tag{2}$$

with

$$\Delta f = \frac{\varepsilon - 1}{2\varepsilon + 1} - \frac{n^2 - 1}{2n^2 + 1}$$

In this equation, c is the light speed and $\hbar$ is Plank's constant divided by 2π. And ε and n are the dielectric constant and the refractive index of solvent, respectively. Thus, the relationship between Stoke's shift ($\Delta\nu$) and orientation polarizability (Δf) of two samples are plotted in Fig. 6. One can see that line **1** (represented for monobranch **1**) and line **2** (represented for multibranch **2**) are parallel to each other, which implies that both of them have the same slopes, namely, the same values of $\Delta\mu_{ge}^2/c\hbar\alpha^3$, as shown in Eq. (2). Therefore, we can deduce that multibranch **2** possesses much larger dipole moment difference ($\Delta\mu_{ge}$) than monobranch **1** because multibranch **2** shows much bigger size, i.e., much larger the cavity radius (α) in comparison with monobranch **1**. Clearly, multibranch **2** undergoes much larger excited charge redistribution leading to strong electron coupling and excited electron delocalization.

4. Conclusions

Two new triphenylamine derivatives, (*N*-(4-(4-(diphenylamino)styryl)phenyl)acetamide) (monobranch **1**) and (*N*-(4-(4-(bis(4-(4-(diphenylamino)styryl)phenyl)amino)styryl)phenyl) acetamide) (multibranch **2**) have been synthesized to investigate the influence of branching structure upon TPA properties. It is interesting to find that multibranch **2** has larger TPA cross-section as high as 1562 GM, showing 17-fold increase in comparison with monobranch **1** (91 GM). Strong electron coupling effect within individual branches, derived from planar and flexible configuration of molecular skeleton, has significant contribution to the cooperative enhancement TPA, which is confirmed by Lippert–Mataga equation and linear optical properties including absorption, stead-fluorescence and time-resolved fluorescence spectra.

Acknowledgements

The authors are grateful to the National Natural Science Foundation of China (Grant Nos. 50273024, 50673070 and 20543001), the Foundation for the Author of National Excellent Doctoral Dissertation of PR China (FANEDD, Grant No. 200333) and International Cooperation Project of Suzhou (SWH 0616) for financial support.

References

[1] Denk W, Strickler JH, Webb WW. Two-photon laser scanning fluorescence microscopy. Science 1990;248:73–6.

[2] Cumpston BH, Ananthavel SP, Barlow S, Dyer DL, Ehrlich JE, Erskine LL, et al. Two-photon polymerization initiators for three-dimensional optical data storage and microfabrication. Nature 1999;398:51–4.

[3] Kawata S, Sun H-B, Tanaka T, Takada K. Finer features for functional microdevices. Nature 2001;412:697–8.

[4] Straub M, Nguyen LH, Fazlic A, Gu M. Complex-shaped three-dimensional microstructures and photonic crystals generated in a polysiloxane polymer by two-photon microstereolithography. Optical Materials 2004;27:359–64.

[5] Parthenopoulos DA, Rentzepis PM. Three-dimensional optical storage memory. Science 1989;245:843–5.

[6] Bhawalkar JD, He GS, Park C-K, Zhao CF, Ruland G, Prasad PN. Efficient, two-photon pumped green upconverted cavity lasing in a new dye. Optics Communications 1996;124:33–7.

[7] He GS, Xu GC, Prasad PN, Reinhardt BA, Bhatt JC, Dillard AG. Two-photon absorption and optical-limiting properties of novel organic compounds. Optics Letters 1995;20:435–7.

[8] Bhawalkar JD, Kumar ND, Zhao CF, Prasad PN. Two-photon photodynamic therapy. Journal of Clinical Laser Medicine and Surgery 1997;15:201–4.

[9] Albota M, Beljonne D, Bredas J-L, Ehrlich JE, Fu J-Y, Heikal AA, et al. Design of organic molecules with large two-photon absorption cross-sections. Science 1998;281:1653–6.

[10] Mongin O, Porres L, Moreaux L, Mertz J, Blanchard-Desce M. Synthesis and photophysical properties of new conjugated fluorophores designed for two-photon-excited fluorescence. Organic Letters 2002;4:719–22.

[11] Chung S-J, Kim K-S, Lin T-C, He GS, Swiatkiewicz J, Prasad PN. Cooperative enhancement of two-photon absorption in multi-branched structures. Journal of Physical Chemistry B 1999;103:10741–5.

[12] Yoo J, Yang SK, Jeong M-Y, Ahn HC, Jeon S-J, Cho BR. Bis-1,4-(*p*-diarylaminostryl)-2,5-dicyanobenzene derivatives with large two-photon absorption cross-sections. Organic Letters 2003;5:645–8.

[13] Brousmiche DW, Serin JM, Frechet MJ, He GS, Lin TC, Chung SJ, et al. Fluorescence resonance energy transfer in novel multiphoton absorbing dendritic structures. Journal of Physical Chemistry B 2004;108:8592–600.

[14] Pond SK, Rumi M, Levin MD, Parker TC, Beljonne D, Day MW, et al. One- and two-photon spectroscopy of donor–acceptor–donor distyrylbenzene derivatives: effect of cyano substitution and distortion from planarity. Journal of Physical Chemistry A 2002;106:11470–80.

[15] Ventelon L, Morel Y, Baldeck P, Moreaux L, Mertz J, Blanchard-Desce M. Novel quadrupolar extended biphenyl derivatives with enhanced nonlinear absorptivities for optical limiting applications. Nonlinear Optics Principles Materials Phenomena and Devices 2001;27:249–58.

[16] Porres L, Mongin O, Blanchard-Desce MH, Ventelon L, Barzoukas M, Moreaux L, et al. Molecular engineering of nanoscale quadrupolar chromophores for two-photon absorption. Proceedings of the SPIE – The International Society for Optical Engineering 2003;4797:284–92.

[17] Blanchard-Desce Mireille (Synthese et Electrosynthese Org., Campus Scientifique de Beaulieu, Universite de Rennes 1), Ventelon L, Moreaux L, Mertz J. Optimization of quadrupolar chromophores for molecular two-photon absorption. Synthetic Metals 2002;127:17–21.

[18] Cho BR, Son KH, Lee SH, Song Y-S, Lee Y-K, Jeon S-J, et al. Two photon absorption properties of 1,3,5-tricyano-2,4,6-tris(styryl)benzene derivatives. Journal of the American Chemical Society 2001;123:10039–45.

[19] Cho BR, Piao MJ, Son KH, Lee SH, Yoon SJ, Jeon S-J, et al. Nonlinear optical and two-photon absorption properties of 1,3,5-tricyano-2,4,6-tris(styryl)benzene-containing octupolar oligomers. Chemistry – A European Journal 2002;8:3907–16.

[20] Hua JL, Li B, Meng FS, Ding F, Qian SX, Tian H. Two-photon absorption properties of hyperbranched conjugated polymers with triphenylamine as the core. Polymer 2004;45:7143–9.

[21] Wang XM, Yang P, Xu GB, Jiang WL, Yang TS. Two-photon absorption and two-photon excited fluorescence of triphenylamine-based multibranched chromophores. Synthetic Metals 2005;155:464–73.

[22] Wang XM, Yang P, Li B, Jiang WL, Huang W, Qian SX, et al. Two-photon absorption of new multibranched chromophore with dibenzothiophene core. Chemical Physics Letters 2006;424:333–9.

[23] Drobizhev M, Karotki A, Dzenis Y, Rebane A, Suo Z, Spangler CW. Strong cooperative enhancement of two-photon absorption in dendrimers. Journal of Physical Chemistry B 2003;107:7540–3.

[24] Shen L, Wang XM, Li B, Jiang WL, Yang P, Qian SX, et al. Two-photon absorption properties of substituted porphyrins. Journal of Porphyrins and Phthalocyanines 2006;10(3):160–6.

[25] Ren Y, Qian X, Tao XT, Wang L, Yu XQ, Yang JX, et al. Novel multibranched organic compounds with enhanced two-photon absorption benefiting from the strong electronic coupling. Chemical Physics Letters 2005;414:253–8.

[26] Lahankar S-A, West R, Varnavski O, Xie X-B, Goodson T, Sukhomlinova L, et al. Electronic interactions in a branched chromophore investigated by nonlinear optical and time-resolved spectroscopy. Journal of Chemical Physics 2004;120:337–44.

[27] Zhou X, Feng JK, Ren AM. Theoretical investigation on the one- and two-photon absorption properties of multi-branched oligomers with truxenone center and fluorene branches. Chemical Physics Letters 2004;397:500–9.

[28] Sun YH, Zhao K, Wang CK, Luo Y, Ren Y, Tao XT, et al. Two-photon absorption properties of multi-branched bis-(styryl)benzene based organic chromophores. Theochem 2004;682:185–9.

[29] Wang XM, Zhou YF, Yu WT, Wang C, Fang Q, Jiang MH. Two-photon pumped lasing stilbene-type chromophores containing various terminal donor groups: relationship between lasing effciency and intramolecular charge transfer. Journal of Materials Chemistry 2000;10:2698–703.

[30] Huang ZZ, Wang XM, Li B, Lv CG, Xu J, Jiang WL, et al. Two-photon absorption of new multibranched chromophores based on bis(diphenylamino)stilbene. Optical Materials 2007;29:1084–90.

[31] Xu C, Webb WW. Measurement of two-photon excitation cross-sections of molecular fluorophores with data from 690 to 1050 nm. Journal of the Optical Society of America B Optical Physics 1996;13:481–91.

[32] Wang XM, Zhou YF, Zhou GY, Jiang WL, Jiang MH. Symmetric, asymmetric charge transfer process of substituted stilbene or its analogues and the one-photon/two-photons excited emission. Bulletin of the Chemical Society of Japan 2002;8:1847–54.

[33] Sarkar N, Das K, Nath DN, Bhattacharyya K. Twisted charge transfer process of Nile Red in homogeneous solution and in faujasite zeolite. Langmuir 1994;10:326–9.

[34] Wang XM, Wang D, Zhou GY, Yu WT, Zhou YF, Fang Q, et al. Symmetric and asymmetric charge transfer process of two-photon absorbing chromophores: bis-donor substituted stilbenes, and substituted styrylquinolinium and styrylpyridinium derivatives. Journal of Materials Chemistry 2001;11:1600–5.

[35] Andruleviciute V, Lazauskaite R, Grazulevicius JV. Synthesis and photopolymerization of new triphenylamine-based oxiranes. Designed Monomers and Polymers 2007;10:105–18.

[36] Sander R, Stuempflen V, Wendorff JH, Greiner A. Synthesis, properties, and guest–host systems of triphenylamine-based oligo(arylenevinylene)s: advanced materials for LED applications. Macromolecules 1996;29:7705–8.

[37] Lupton JM, Samuel IDM, Burn PL, Mukamel S. Control of intrachromophore excitonic coherence in electroluminescent conjugated dendrimers. Journal of Physical Chemistry B 2002;106:7647–53.

[38] Drobizhev M, Rebane A, Sigel C, Elandaloussi EH, Spangler CW. Picosecond dynamics of excitations studied in three generations of new 4,4′-bis(diphenylamino)stilbene-based dendrimers. Chemical Physics Letters 2000;325:375–82.

[39] Varnavski O, Goodson T. Femtosecond fluorescence dynamics and molecular interactions in a water-soluble nonlinear optical polymeric dye. Chemical Physics Letters 2000;320:688–96.

[40] Heller CM, Campbell IH, Laurich BK, Smith DL, Bradley DDC, Burn PL, et al. Solid-state-concentration effects on the optical absorption and emission of poly(*p*-phenylene vinylene)-related materials. Physical Review B Condensed Matter 1996;54:5516–22.

[41] Bazan GC, Oldham Jr WJ, Lachicotte RJ, Tretiak S, Chernyak V, Mukamel S. Stilbenoid dimers: dissection of a paracyclophane chromophore. Journal of the American Chemical Society 1998;120:9188–204.

[42] Liu GH, Yang P, Jiang WL, Guo XZ, Xu GB, Jiang XZ, et al. Synthesis and strong two-photon absorption of carbazole derivatives: NT-G1 and NO-G1. Functional Materials 2005;5:600–3 [in Chinese].

[43] Lu Y, Hasegawa F, Goto T, Ohkuma S, Fukuhara S, Kawazu Y, et al. Highly sensitive two-photon chromophores applied to three-dimensional lithographic microfabrication: design, synthesis and characterization towards two-photon absorption cross-section. Journal of Materials Chemistry 2004;14:75–80.

[44] Polyzos I, Tsigaridas G, Fakis M, Giannetas V, Persephonis P, Mikroyannidis J. Two-photon absorption properties of novel organic materials for three-dimensional optical memories. Chemical Physics Letters 2003;369:264–8.

[45] Day D, Gu M. Formation of voids in a doped polymethylmethacrylate polymer. Applied Physics Letters 2002;80:2404–6.